# SHAPE AND SIZE FROM THE MIST
## *A Deformable Model for Particle Characterization*

Anders Dahl[†], Thomas Martini Jørgensen[‡], Phanindra Gundu[‡], Rasmus Larsen[†]

*Technical University of Denmark, DTU Informatics Lyngby[†], DTU Photonics Risø[‡], Denmark*
*abd@imm.dtu.dk, tmjq@risoe.dtu.dk, phag@risoe.dtu.dk, rl@imm.dtu.dk*

Abstract:     Process optimization often depends on the correct estimation of particle size, their shape and their concentration. In case of the backlight microscopic system, which we investigate here, particle images suffer from out-of-focus blur. This gives a bias towards overestimating the particle size when particles are behind or in front of the focus plane. In most applications only in-focus particles get analyzed, but this weakens the statistical basis and requires either particle sampling over longer time or results in uncertain predictions. We propose a new method for estimating the size and the shape of the particles, which includes out-of-focus particles. We employ particle simulations for training an inference model predicting the true size of particles from image observations. This also provides depth information, which can be used in concentration predictions. Our model shows promising results on real data with ground truth depth, shape and size information. The outcome of our approach is a reliable particle analysis obtained from shorter sampling time.

## 1 INTRODUCTION

Visual inspection of particles is often essential for optimizing industrial processes. Examples can be particles in a dissolution, as for instance in a fermentation process, or particles in gas, such as the coal particles from a power plant. A vision-based system can provide knowledge about particle distribution, size and shape, and these parameters are important for process control. The choice of the analysis method and the image quality affects the process control, and as a result both the analysis and image acquisition should be chosen carefully.

The motivation of our work is an industrial endoscopic inspection system equipped with a probe that can be placed inside the process[1]. Images are acquired from the tip of the probe, which also contains a light source placed in front of the camera. The resulting camera setup depicts particles as shadows, see Figure 1. Visual appearance of the particles depends on the optical properties of the camera setup,

the distance of the particles to the focus plane, and the physical reflectance properties of the particles. The depth of field of the camera optics is narrow and the particles get blurred as they move away from the focus plane, which introduces uncertainty of the particle characterization, see Figure 2. Employing a strategy where only in-focus particles are analyzed can be a good solution, but in situations with few particles or short inspection time this approach will give an uncertain estimate due to low sample size. As a consequence it can be necessary to perform the analysis of the blurred particles as well.

**Deblurring** In a linear system the image formation can be described as the linear convolution of the object distribution and the point spread function (PSF). Hence, to reduce the blur from out of focus light, ideally the mathematical process of deconvolution can be applied. However, noise can easily be enhanced if one just implements a direct inverse operation, so the inverse has to be regularized. Different regularizers can be employed, for example iteratively deconvolving the image (Lucy, 1974), (Richardson, 1972), or using a Wiener filter (Wiener, 1964). Alternatively,

---

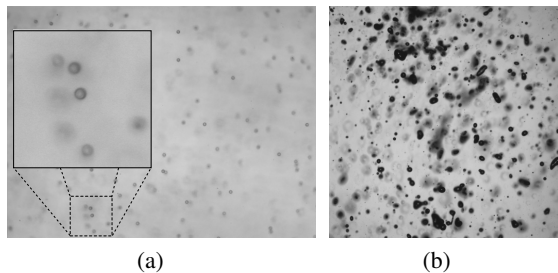[1]PROVAEN – Process Visualisation and Analysis ENdoscope System (EU, $6^{th}$ Framework)

Figure 1: Examples of particle images. (a) spherical transparent particles all 25 $\mu$m in diameter, and (b) a typical image to be analyzed depicting spray particles.
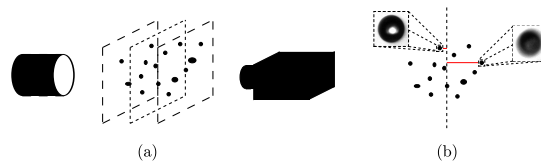


Figure 2: Illustration of the particles relative to the focus plane. (a) particles in the 3D volume (b) can potentially appear as a function of the distance to the focus plane.

a maximum entropy solution can be chosen, which aims at being mostly consistent with data (Narayan and Nityananda, 1986), (Starck et al., 2002). These methods assume a known PSF. When this is not the case, blind deconvolution can in some cases be applied recovering both the PSF and the deconvolved image. Typically this is solved by an optimization criterion based on known physical properties of the depicted object (Kundur and Hatzinakos, 1996).

These methods are based on the assumption of a known – possibly space-dependent – PSF for the whole image. For many optical systems it is difficult to calculate a theoretical PSF with sufficiently accuracy to be used for deconvolution. Also it can be quite difficult to measure it experimentally with sufficient resolution and accuracy. In our case the particles of concern are illuminated from the back and in this respect it resembles the case of bright light microscopy. Such an imaging system is not exactly a linear device but in practice it is almost so. However, in the bright field setting the "simple" PSF is compounded by absorptive, refractive and dispersal effects, making it rather difficult to measure and calculate it.

Methods for local image deblurring, which is needed for our problem, include iteratively estimating the blur kernel and updating the image accordingly in a Bayesian framework (Shan et al., 2008). Another approach is to segment the image and estimate an individual blur kernel for the segments (Cho et al., 2007; Levin, 2007). Blur also contains information about the depicted objects. This has been used by (Dai and Wu, 2008; Shan et al., 2007), where they obtain motion information by modeling blur. With a successful deblurring, e.g. based on one of these methods, we will still have to identify the individual particles. Instead, we suggest here to build a particle model.

**Particle modeling** Most particles have a fairly simple structure, typically being convex and close to circular or elliptical. This observation can be used for

designing a particle model. In (Fisker et al., 2000) a particle model is build for nanoparticles based on images obtained from an electron microscope. An elliptical model is aligned with the particles by maximizing the contrast between the average intensity of the particle and a surrounding narrow band. Particles in these images are naturally in focus.

Ghaemi *et al.*(Ghaemi et al., 2008) analyze spray particles using a simple elliptical model. However, only in-focus particles are analyzed, and out of focus particles are pointed out as a cause of error. In addition, they mention the discretization on the CCD chip to be problematic, and argue that particles should be at least 40-60 pixels across to enable a good shape characterization.

Under the assumption that images are smooth and by modeling the out of focus blur, we are able to experimentally show that we can obtain reliable shape and size information from particles smaller than 40-60 pixels in diameter. The main contribution of this paper and the basis for our experiments is a particle model, which is used for characterizing particle shape, size and blur. In Section 2 we describe our particle model and how it can be used for particle characterization. We experimentally validate the particle model in Section 3. Lastly, in Section 4 we discuss the obtained results, and we conclude the work in Section 5.

## 2 METHOD

The goal of the proposed method is to obtain information about the true size and shape of an out of focus particle. Our idea is to learn particle appearance from observations of particles with known position relative to the focus plane. By comparing the appearance of an unknown particle to the training set, we can predict how the particle would appear, if it was in focus. As a result we obtain information about the true particle size and shape.

To facilitate this, the particles must be characterized in a way that describes the appearance as a function of blur well. Furthermore, particles should be easy to
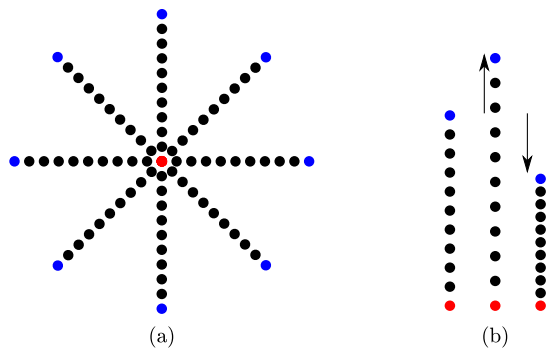
(a)                                        (b)

Figure 3: Intensity sampling with the particle model. Radial sampling pattern of our model with 10 sampling steps from the center point, marked with red, to the end of the radial line marked with blue. There are 8 radial sampling lines in this example (a). Each radial sampling line can be deformed by stretching or compressing the line while keeping equal distance between the sampling points (b). This stretch of the individual sampling lines is what deforms our model.

compare. We will now give a short description of how particles are depicted, and then explain the details of our particle model and descriptor. Finally we describe the statistical model for depth estimation.

**Experimental setup**  The particle analysis is based on backlight where the particles appear as shadows. Real image examples are shown in Figure 1 and Figure 2 illustrates the experimental setup. Notice that all particles in Figure 1(a) are the same size of $25\mu$m, but the blur makes them appear very different. Out of focus blur occurs both in front and behind the focus plane, but it is hard to tell if an observed particle is in front or behind, because the blur looks the same. As a consequence we have chosen to model the particles as a function of absolute distance to the focus plan, which is shown in Figure 2. In Section 3 we experimentally show that these are reasonable assumptions.

**Particle analysis model**  The objective is to design a model that encodes information about the particle's size, shape and blur. Our model is based on the observation that particles show close to radial symmetry. If we sample along line segments from the center of the particle, we expect to see the same intensity pattern or a scaled version of this pattern. This is the idea that we base our particle model on, which is illustrated in Figure 3.
Our particle prediction is based on the following

$$\mathbf{Y} = [s_t, r_t, d_t]^T = f(c_o, r_o, I_o), \qquad (1)$$

where $(c_o, r_o, I_o)$ are the observed spatial position, shape and image appearance respectively, $f$ is the
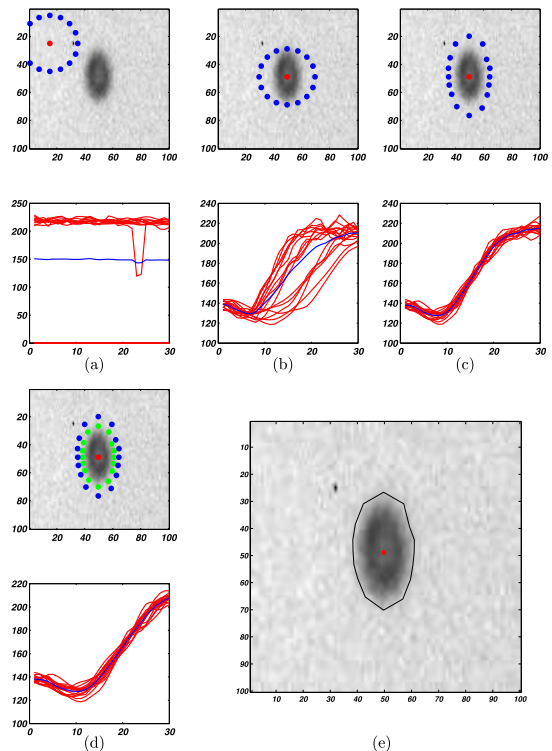


Figure 4: Particle alignment and deformation. The image shows the particle, the red dot is the center, and the blue dots are the radial endpoints. The red curves show the intensity pattern along the individual radial lines and the blue is the average. The blob is initialized in (a), translated in (b), deformed in (c), the size is found in marked with green points (d) resulting in the segment in (e). Note that despite a very poor initial alignment the model finds the object very precisely. Also note how uniform the intensity pattern becomes by deformation.

function mapping observations to the vector $\mathbf{Y}$ containing the model prediction $(s_t, r_t, d_t)$, which is the true size, shape and distance to the focus plane. We will now give the details of the particle model and then explain how the parameters of this model are used for predicting the particle characteristics.
We sample $n$ radial lines form the center coordinates $c_o$ placed with equal angle around the center point. A particle descriptor is obtained by sampling the image intensity along these radial lines at $m$ equidistant positions relative to the lengths of the radial lines. This intensity descriptor is denoted $I_o$. The length of the radial lines are stored in the $r_o$ vector, which characterizes the particle shape.

**Alignment with image data**  Adapting the model to the image observations is done in two steps. First by changing the center position, which translates the model, and secondly by changing the length of the

radial lines, which deforms the shape of the model. Both operations will change the intensity descriptor, which is utilized for finding an optimal particle characterization. As a preprocessing step for noise removal we convolve the image with a Gaussian kernel with standard deviation $\sigma$.

The particle model has to be initialized by a rough estimate of the particle size and position, e.g. using scale space blob detection, see (Lindeberg, 1994). To obtain the center position of a particle we use an optimization criterion based on radial symmetry and intensity variance. The reasoning for the first criterion is that particles are typically radially symmetric. Based on that we initiate our particle model with radial lines of equal length. We expect the radial lines to have highest similarity when they are sampled from the particle center, also for particles that are not spherically shaped. The variation criterion is based on the fact that the intensity descriptor has high variation when sampled on a particle and low otherwise. This turns out to be very important for the robustness of the alignment. The minimization problem becomes

$$\underset{c}{\operatorname{argmin}}\left(\eta\big(\sum_{i=1}^{n}||I_i-\bar{I}||\big)-\xi\sigma_{\bar{I}}\right), \qquad (2)$$

where $\bar{I}$ is the mean intensity descriptor, and the sum of normed descriptor differences is weighed by $\eta$. $\sigma_{\bar{I}}$ is the standard deviation of the mean descriptor, which is weighed by $\xi$. This alignment is optimized by simple gradient decent, by moving in the steepest decent direction until an optimum is reached. The procedure is repeated with finer step size, until a desired precision is obtained.

After an optimal particle position has been found, the particle shape is optimized to the image data by changing the length of the radial sampling lines

$$\underset{r}{\operatorname{argmin}}\left(\sum_{i=1}^{n}||I_i-\bar{I}||\right), \qquad (3)$$

hereby minimizing the difference between the average descriptor and the individual radial descriptors. This optimization is done similarly to the positioning, also using gradient decent and refining the step size when a minimum is reached. The length of the final radial lines are normalized to sum to the same as original radial lines lengths.

The particle model results in an observed characterization as follows

$$\mathbf{x}=\{c_o,r_o,I_o\}, \qquad (4)$$

containing the center position denoted $c_o$ which is a 2D vector, the length of the radial line segments denoted $r_o$ which is a $n$-dimensional vector, and the in-

tensity pattern $I_o$ which is $m$-dimensional. It is estimated as the mean $I_o = \frac{1}{n}\sum_{i=1}^{n}I_i'$, where $I_i'$ is the radial pattern of line segment $i$. It should be noted that the difference between the line patterns have been minimized, so we model the remaining difference as noise, and as a result the averaging will smooth this noise and make the estimate robust.

Modeling the particle will create an independent characterization of the size, shape and blur, which is illustrated in Figure 3. Particle shape is encoded in the length of the radial line segments, and the particle size can be obtained from a combination of the radial intensity pattern and the length of the line segments. The intensity pattern $I_o$ has a shape that bends off to become indistinguishable from the background, see Figure 4, and the particle boundary is estimated at this point. We found a function of the total variation to be good way of estimating this. We estimate the total variation as the sum of absolute differences of $I_o$ and we obtain the distance as

$$r_o = \underset{j}{\operatorname{argmax}}\left(\frac{\sum_{i=1}^{m-j}||I_{o_i}-I_{o_{i+1}}||-c}{j\sum_{i=1}^{m-1}||I_{o_i}-I_{o_{i+1}}||}\right)$$
$$j\in\{1,...,m-1\}, \qquad (5)$$

which is the normed total variation. The constant $c$ influences the estimated size of the particle.

**Statistical analysis** The blur is encoded in the radial pattern descriptor ($I_o$), which we use as input for estimating the distance to the focus plane. We use a linear ridge regression to obtain the depth. The model is $d_f = I_o\beta^r$, where $\beta^r$ is the coefficients of the regression model. We obtain the model parameters from a training set with known distance to the focus plane by solving $\beta^r = (I_o^T I_o + \lambda\mathbf{I})^{-1}I_o^T d_t^*$, where $d_t^*$ is the distance of the training data. See for example (Hastie et al., 2005) for a detailed description of ridge regression.

Table 1: Model parameters.

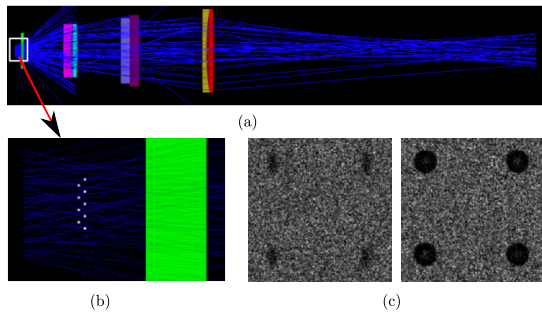| Parameter | Value |
|---|---|
| Radial lines ($n$) | 8 |
| Sampling steps ($m$) | 40 |
| Sampling distance (pixels) | 30 |
| Length constant ($c$) | 0.35 |
| Gaussian blur - simulated ($\sigma$) | 5 |
| Gaussian blur - real ($\sigma$) | 1 |
| Radial similarty ($\eta$ - Equation 2) | 1 |
| Variance weight ($\xi$ - Equation 2) | 4000 |

Figure 5: Optical simulation in Zemax. (a) back illumination with a diffuse light source of 2 mm$^2$ with wavelengths of 480-650 nm with transparent particles. (b) zoom on the particles and (c) examples of 50 $\mu$m out of focus ellipsoid particels (50 $\mu$m $\times$ 16.7 $\mu$m) and spherical in focus particles (50 $\mu$m).
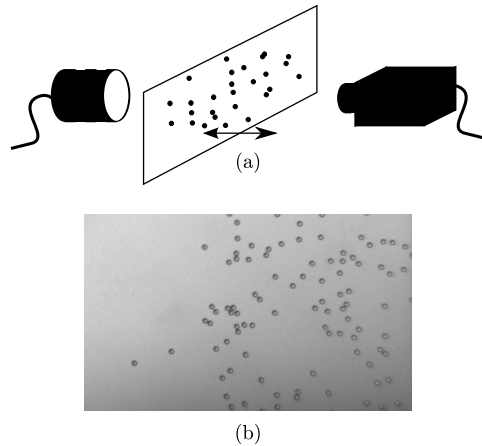


Figure 6: Setup for acquiring real data. (a) particles placed between glass sheets that can be moved relative to the camera. (b) image example with LED back illumination and 25 $\mu$m spherical transparent particles.

# 3 EXPERIMENTS

In this section we will experimentally show the performance of our particle model. We want to investigate the precision and accuracy of our model. By precision we mean how good our model is in predicting the true size, shape and particle depth. The accuracy refers to variation in the model predictions. The experiments are conducted in relation to size estimation, shape estimation and the particles distance to the focus plane. For these experiments we chose the parameter shown in Table 1. Furthermore, we investigate the robustness of the input parameter choices, which concerns number of radial lines, number of sampling steps, sampling distance, optimization weights, see Equation 2, and the initial position and size estimates of the particles.

**Data** The endoscopic probe consists of three doublets with different powers separated as shown in Figure 5. The distance between the object plane (particles) and the first optical element, which is a cover plate, is just 1 mm. The separations between the optical elements up to the CCD is so maintained and optimized to provide a magnification of 6. The design is performed in Zemax optical design software. The total track length from object to image (particles to CCD) is 25 cm and the optical resolution of the system is 2 microns. The entire visible wavelength region is used to optimize this system (480-650 nm). The depth of focus at the object side is computed to be +/- 75 microns when defined by a drop of more than 90% of the modulation transfer function. To incorporate the real situation of illumination with back light of spherical and ellipsoidal particles, modeling is done in a non-sequential mode in Zemax, which can

handle diffuse light and 3D particles. The diffuse light source is located a few millimeters behind the particles and emits light in the specified wavelength range randomly over a 15 degrees angle. The particles used are transparent with refractive index of 1.6 at 555 nm wavelength. Several million rays per simulation were used to generate a single image with particles. Imaging is done using a CCD array with 4 Megapixels of 7 micron pitch.

The real data set consists of particles in water suspension placed between two glass sheets, which have been moved with $\mu$m precision relative to the focus plane. 25 $\mu$m particles are shown in Figure 6.

**Size experiment** In this experiment we investigate the robustness of our size estimation. We have both tested the mean value and standard deviation of the estimated size, and how it depends on the distance to the focus plane. The results are shown in Figure 7. The first three graphs (a)-(c) shows a relative size estimate as a function of distance to the focus plane, and each curve shows an individual size. There is a general bias towards overestimating the size of particles that are out of focus and small particles are also somewhat overestimated. The model is not capable of handling very large size changes, and gives an erroneous prediction for particle scaled to 25% size. This is due to the fixed parameter setting where the sampling is too coarse to identify the small particles. Size variation is obtained by scaling the images.

Figure 8 illustrates the robustness to inaccurate spatial initialization. The model will only fail in finding a good center approximation if it is initialization far from the particle and especially if it is done diagonal.
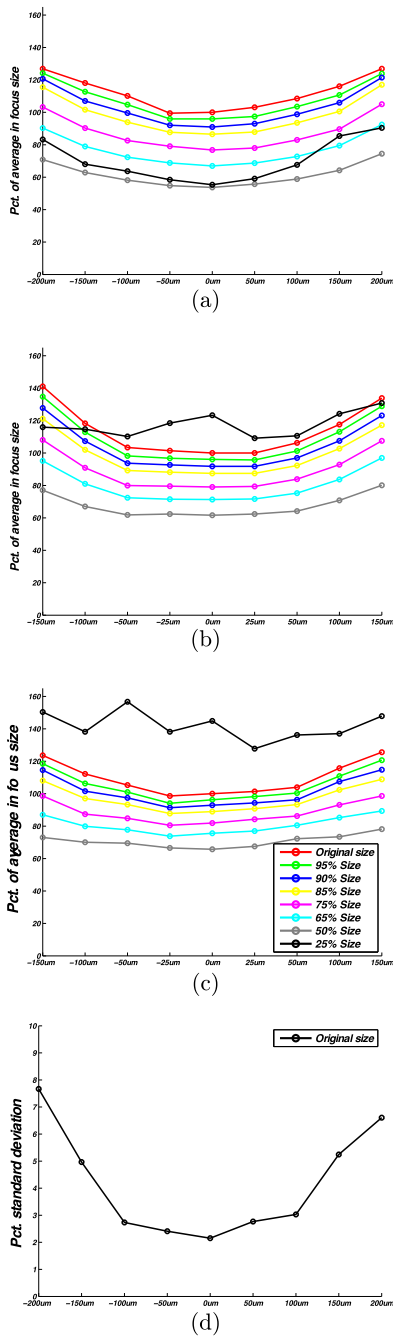
(a)

(b)

(c)

(d)

Figure 7: Experiment with change of size. The horizontal axis of (a)-(c) shows the average radial distance relative to the in focus particle of original size. Standard deviation of the size estimate in percent of the original (d). Note the bias towards overestimation of size and less certainty as a function of out of focus.

**Shape experiment** The purpose of this experiment is to investigate how the model deforms to adapt to non-spherical particles. The results are shown in Fig-
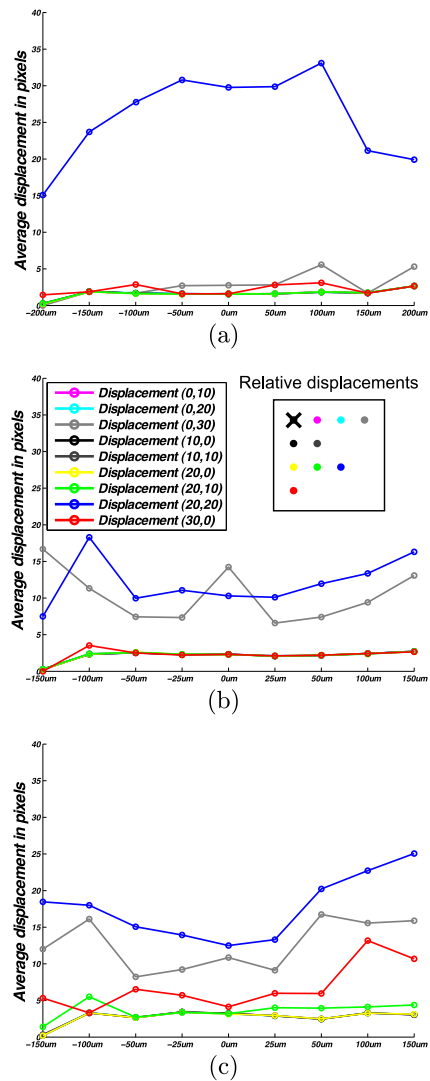


(a)

(b)

(c)

Figure 8: Experiment for testing robustness to wrong spatial initialization of particle. Vertical axis is the average distance in pixels to the true position and horizontal axis is the particle distance to the focus plane. A 50 $\mu$m particle has a radius of about 17 pixels. Experiments have been carried out for simulated particles, which are spherical (a), ellipsoids ($1 \times 2$) (b), and ellipsoids ($1 \times 3$) (c). Ellipsoids have the major axis vertical. The displacements are schematically shown in (b). Each displacement step is 10 pixels.

ure 9, where the relation between the horizontal and vertical line segments are plotted as a function of particle distance to the focus plane. The particles does not adapt completely to the expected shape, and there is a tendency for out of focus particles to be more circular than in focus particles. Despite the particle shape is not found exactly from the experiment, this can be inferred by regression, which we will show next.
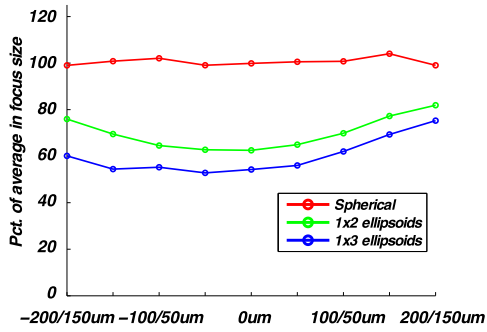
Figure 9: Shape experiment. The horizontal axis is the relation between the vertical and horizontal line segments from our particle model, corresponding to the minor and major axis in the simulated ellipsoids. The true relation for the red curve would be 1, the green curve would be 0.5 and the blue curve would be 0.33.

Table 2: Regression model. Regression has been done for both simulated and real data. There were 25 particles in the simulated data and 82 particles in the real data set. The reported numbers are the standard deviation of the absolute errors of the regression, and the size range of the numbers. The columns are distance to the focus plane (Distance FP), average radial line length (Size), relation between the radial and horizontal line lengths (Shape).

| Simulated data | | | |
|---|---|---|---|
| | Distance FP | Size | Shape |
| Std. | $14.20\mu$m | $0.8921\mu$m | 0.0357 |
| Range | $0-200\mu$m | $33.3-50\mu$m | 0.33-1.0 |
| Real data | | | |
| | Distance FP | | |
| Std. | $21.69\mu$m | | |
| Range | $0-180\mu$m | | |

**Regression experiment** Results from our regression experiment is shown in Table 2. The regression is performed using ridge regression with $\lambda = 10^{-5}$. We divided our data set into approximately half training and half test sets, which was 12 particles from the simulated set for training and 13 particles for test, from each image. In the real data set, we have 82 depicted particles, and the split was 41 in each group. We had 27 simulated images, giving 675 observations for the simulation set. In the observed data set we have 82 particles in 9 images giving 738 observations. The results are obtained from 100 random splits in test and training data. We use the mean radial descriptor ($I_o$) and the length for each line segment ($r_o$) as input to our regression, see Equation 4.

In the simulated data we perform a regression for both distance to the focus plane, particle size, and shape, which is the relation between the major and minor axis. The obtained results show precise predictions, indicating that this characterization is adequate for reliable particle modeling. For the real data we also obtained satisfactory prediction of the distance to the focus plane, but with about 50% lower precision.

## 4  DISCUSSION

The data for our experiment is based on LED illumination, both what is used in the real data, and what is simulated. This is a rather cheep solution, and if it can provide satisfactory results, it will be a cost effective solution. But the rather diffuse illumination from the LEDs could be replaced by collinear laser, which will give much higher particle contrast, and therefore potentially improved performance. Wether this will give larger depth of field or just improved predictions

is for future investigations to show.

The size experiment illustrates how robust our particle model is to the initialization. With the same set of parameters, it is capable of handling up to 50% scale change. But with an initialization, using for example scale space blob detection, this should be adequate to adjusting the parameters to obtain a precise particle characterization.

Scaling images for size variation does not account for the change i optical properties of smaller particles. We know that smaller particles in back-illumination change appearance caused by scattering effects like refraction and defraction, and this requires further investigations to verify that our model will be able to characterize these particles. The appearance change will result in blurred particles, which our particle model handles fine. As a consequence the main focus should be on weather the regression model can predict the true size. Our regression experiment indicates that this should be possible.

The shape experiment shows that the model does not adapt precisely to the shape of the particle. This is caused by the Gaussian noise removal, which also blurs the particles making them appear less ellipsoid than they are in reality. The reason for the quite dramatic Gaussian convolution, which actually acts contrary to the deconvolution that we are trying to infer, is the noise level in the simulations. The noise is much larger, than what is seen in the real data, which can be seen by comparing the images in Figure 5 (c) and Figure 6 (b). But even with this high noise level, it was possible to infer the true shape by ridge regression.

Our regression experiment shows that the size, shape, and distance to the focus plane can be inferred using our particle model. This is highly encouraging, because it can help in performing more reliable particle analysis, than by just using the in focus particles,

see e.g. (Ghaemi et al., 2008). The linear ridge regression is a simple procedure, and much more advanced methods exists, which for example can handle non-linearities. This might be relevant for inferring particle information of a larger size range or very small particles, where scattering effects are more pronounced. In this paper we have chosen to primarily focus on the particle model, so we leave this for future investigations.

The data set for our experiments are somewhat limited, and we plan to extend the data in future investigations. This should also include less noisy simulations, which can be obtained from extended simulation time. In addition to more data, we will also investigate how model parameters can be used for predicting properties of real data. This will enable simulations of complicated particle modeling for which it is very hard to obtain ground truth, for example complicated shaped particles or various illumination conditions. From this better analysis setups can be designed, and expected performance can be estimated.

There are no comparative studies between our model and similar approaches, because other procedures are based on modeling in focus particles, see e.g. (Fisker et al., 2000; Ghaemi et al., 2008). The radial sampling lines, which we use in our model, will give much weight to the center part of the particle. How this influences the particle predictions and if this can help for improvements should be investigated.

## 5  CONCLUSION

There are two main contributions of the work presented in this paper. Our first contribution is that we experimentally show that out of focus particles can be modeled reliably, and therefore be included in obtaining information of particle size, shape and distance to the focus plane. This is enabled through our particle model, which is our second contribution. The model is very robust and provides precise predictions of particle characteristics. We hope that this can help in removing some of the mist from particle characterization, and hereby give better performance and system design to particle analysis in the future.

## 6  ACKNOWLEDGEMENTS

## REFERENCES

Cho, S., Matsushita, Y., Lee, S., and POSTECH, P. (2007). Removing non-uniform motion blur from images. In *IEEE 11th International Conference on Computer Vision, 2007. ICCV 2007*, pages 1–8.

Dai, S. and Wu, Y. (2008). Motion from blur. In *Proc. Conf. Computer Vision and Pattern Recognition*, pages 1–8.

Fisker, R., Carstensen, J. M., Hansen, M. F., Bødker, F., and Mørup, S. (2000). Estimation of nanoparticle size distributions by image analysis. *Journal of Nanoparticle Research*, 2(3):267–277.

Ghaemi, S., Rahimi, P., and Nobes, D. (2008). Measurement of Droplet Centricity and Velocity in the Spray Field of an Effervescent Atomizer. *Int Symp on Applications of Laser Techniques to Fluid Mechanics, Lisbon, Portugal, 07-10 July, 2008*.

Hastie, T., Tibshirani, R., Friedman, J., and Franklin, J. (2005). The elements of statistical learning: data mining, inference and prediction. *The Mathematical Intelligencer*, 27(2):83–85.

Kundur, D. and Hatzinakos, D. (1996). Blind image deconvolution. *IEEE signal processing magazine*, 13(3):43–64.

Levin, A. (2007). Blind motion deblurring using image statistics. *Advances in Neural Information Processing Systems*, 19:841.

Lindeberg, T. (1994). *Scale-space theory in computer vision*. Springer.

Lucy, L. B. (1974). An iterative technique for the rectification of observed distributions. *The astronomical journal*, 79(6):745–754.

Narayan, R. and Nityananda, R. (1986). Maximum entropy image restoration in astronomy. *Annual review of astronomy and astrophysics*, 24(1):127–170.

Richardson, W. H. (1972). Bayesian-based iterative method of image restoration. *Journal of the Optical Society of America*, 62(1):55–59.

Shan, Q., Jia, J., and Agarwala, A. (2008). High-quality motion deblurring from a single image. *ACM Transactions on Graphics-TOG*, 27(3):73–73.

Shan, Q., Xiong, W., and Jia, J. (2007). Rotational motion deblurring of a rigid object from a single image. In *IEEE 11th International Conference on Computer Vision, 2007. ICCV 2007*, pages 1–8. Citeseer.

Starck, J. L., Pantin, E., and Murtagh, F. (2002). Deconvolution in astronomy: a review. *Publications of the Astronomical Society of the Pacific*, 114(800):1051–1069.

Wiener, N. (1964). *Extrapolation, Interpolation, and Smoothing of Stationary Time Series*. The MIT Press.

---

[2]http://www.provaen.com/

[3]http://www.dantecdynamics.com/